Order-to-Chaos Transition in Rotational Nuclei

F.S. Stephens, M.A. Deleplanque, I.Y. Lee, A.O. Macchiavelli, D. Ward, P. Fallon, M. Cromaz, R.M. Clark, M. Descovich, R.M. Diamond, and E. Rodriguez-Vieitez

Nuclear Science Division, Lawrence Berkeley National Laboratory, Berkeley, California 94720

(May 3, 2004)

We have studied the narrow (valley-ridge) structure in the γ-ray spectrum following a heavy-ion fusion reaction that produces several ytterbium nuclei. The intensity of this structure can be quantitatively related to the average chaotic behavior in these nuclei and we have traced this behavior from nearly fully ordered to nearly fully chaotic.

PACS numbers: 21.10.Re 23.20.Lv 27.60.+j 27.70.+q

Chaos in quantal systems is not easily defined; however, a great deal of study has gone into comparing quantal systems with classical analogs, *e.g.* Sinai's billiard [1]. The result is some well established criteria for quantal systems that are thought to indicate whether the corresponding classical system would be ordered or chaotic. One of these is the so-called nearest neighbor distribution (NND), *i.e.* the distribution of energy separations between adjacent states having the same set of conserved quantum numbers (*e.g.* spin and parity). Another is Dyson and Mehta's Δ_3 statistics [2], which examine the level spacings over a longer energy range. Both of these are based on fluctuations in the level spacings, which get smoothed out as a system becomes chaotic. This smoothing can be understood as level repulsion arising from the mixing of states. Such a mixing depends on the ratio, v/d, where v is the interaction between the levels and d is their energy separation. We believe this ratio can be measured directly and reliably in some rotational nuclei.

Chaos in nuclei has been studied using the NND and Δ_3 statistics, and early results showed that near the neutron binding energy in a number of heavy nuclei ($\sim$8 MeV of thermal excitation energy, E^*) the behavior is essentially chaotic [3]; whereas, near the ground state in such nuclei it is mainly ordered [4]. We would like to study the onset of chaos between these points. The Yb nuclei are in this region of nuclei and we study them using heavy-ion fusion reactions, which bring high angular momentum (up to $\sim 70\hbar$) and excitation energy ($\sim$80 MeV) into the fused system. In these nuclei neutron evaporation quickly brings the average E^* down to about the neutron binding energy, and the angular momentum and remaining E^* are removed in a γ-ray cascade down to the ground state. We study this cascade which covers the range where chaos sets in. The Yb nuclei were chosen because nuclei in this region are deformed and exhibit rotational behavior. The γ-ray cascades in rotational nuclei have regularities that are essential for this analysis.

The physics that generates nuclear γ-ray spectra in heavy nuclei is based on the motion of individual nucleons in the mean field generated by all the nucleons (*e.g.* Nilsson [5]). A residual interaction, v, is added, which is the part of the nucleon-nucleon interaction that is not included in the mean field. In the Yb region, the mean-field states are ordered at very low temperatures (near the yrast states) [6] and as a result they each have distinctive rotational properties (emit γ rays of a characteristic energy), together with associated quantum numbers. With increasing E^* the separation between states, d, becomes small and the residual interaction mixes these states (compound damping) over an energy region whose width is called the spreading width, Γ_μ. It is this mixing that generates the order-to-chaos transition we are discussing. The rotational properties are then also mixed (damped) so that each level now emits a broad spread of γ rays whose width is the rotational damping width, Γ_{rot} [7]. It has been recognized for some time that this rotational damping can provide an observable signal for the onset of chaos [6,8–10].

The relationship between these two types of damping is illustrated in Fig. 1. In the region of mixed levels a level (of spin, I) with three components is shown on the right side of Fig. 1. Each of these components emits rotational γ rays having different energies. The level can then emit γ rays having any of these energies, which generates a distribution of γ-ray energies, whose width is Γ_{rot}. However, a new feature noticed by Matsuo [8] is that the compound damping can also show up in these spectra. This is illustrated on the left side of Fig. 1, where two of the components are schematically spread over three final states. The width of this distribution is Γ_μ, which, in the E^* range we are discussing, is generally smaller than Γ_{rot}, as illustrated. It is also possible that the final state is unmixed as illustrated by the third component and this results in a transition with a sharp (unspread) energy characteristic of the well known discrete bands near the ground state. It would be difficult to separate these components in the full spectrum.

However, in a coincidence spectrum the first γ ray (the "gate") will come in via one of the three components as illustrated in Fig. 1. The level can then decay via any of the components, but if it decays by the same (entry) component, it will have a narrow energy correlation characteristic of that component: either unspread (discrete) or spread only by the distribution of the final states, Γ_μ. If it decays via either of the other two components, the

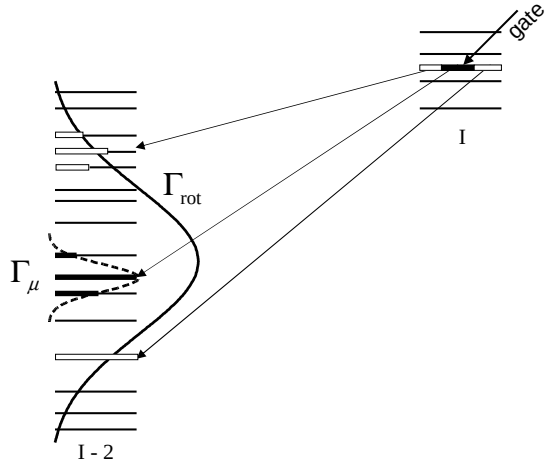

FIG. 1. A sketch of the mixed levels and transitions involved in rotational and compound damping. A gate is shown populating one component of a level having spin, I.

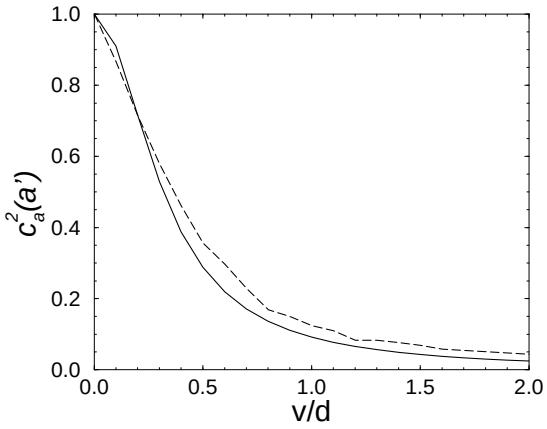

FIG. 2. The relationship of $c_a^2(a')$ to v/d is shown for Eq. 1 (solid line) and the random matrix (dashed line).

width will be comparable to Γ_{rot}. Thus, if the components have equal amplitudes, the probability for the narrow structure, P_{nar}, will be one third and that for Γ_{rot} will be two thirds. This sensitivity to the complexity of the wave function suggests a connection between P_{nar} and chaotic behavior and we want to explore that connection.

Our assumption is that P_{nar} depends on $c_a^2(a')$, the square of the amplitude of the (unmixed) entry component, a, in the (mixed) decaying state, a'; and since any component can be the initial component we are measuring an average value. The spreading of the amplitude of an initial state, a, over an extended range of equally spaced levels has been treated [11] and leads to a Breit-Wigner distribution in energy for the strength, $c_a^2(E)$, with a width, Γ_μ, given by Fermi's golden rule. However, P_{nar} depends on the strength remaining in the initial state (at essentially the initial energy). This is related to the total strength lost to other states, but not specifically to the number of other states nor their energy distribution. With appropriate approximations, we get:

$$1/P_{nar} = 1/c_a^2(a') = 1 + (\pi v/d)^2. \qquad (1)$$

Each measured value of P_{nar} depends on a single variable, v/d, and this is important since v/d is directly related to the chaotic behavior of a system.

To relate v/d to chaotic behavior we diagonalize a symmetric random matrix [12] that gives an ordered behavior (Poisson) for a v/d of zero and a chaotic behavior (Wigner or Gaussian Orthogonal Ensemble, GOE) for a large v/d. The diagonal elements are chosen randomly over an energy interval $-E < 0 < E$ which defines both d and the initial NND (which is Poisson). The off-diagonal elements are chosen randomly from a Gaussian distribution centered at 0 and having an rms value, v. This model implies a relationship between $c_a^2(a')$ and v/d, where $c_a(a')$ is the amplitude of the initial central state in the mixed central state, and this relationship is shown in Fig. 2 compared with that from Eq. 1. The agreement is good, giving us confidence that Eq. 1 and the random matrix are addressing the same problem.

The data were taken [13] using Gammasphere at the LBNL 88-Inch Cyclotron to record γ rays from the reaction of 215 MeV ^{48}Ca projectiles on a 1 mg/cm^2 target of ^{124}Sn. This reaction forms the fusion product, ^{172}Yb, which decays into the product nuclei, ^{168,167,166}Yb, with yields of roughly 20, 40, and 40%, respectively. Events were stored if 5-or-more clean (no hit in the Compton suppressor) γ rays were in coincidence. About 2x10^9 such events were recorded and sorted into a 2D (E_γ-E_γ) matrix. Correlation spectra were generated from the 2D matrix using the COR procedure [14] which subtracts an uncorrelated background from the data. For a gated spectrum this background is the full-projection spectrum normalized to the same area.

Our simulation describes the cascade of γ rays following the fusion reaction and has been previously described [13]. A very brief summary will be given here. The cascade starts from a spin and an E^* randomly selected from distributions based on measured data. The cascade is a competition between E1 statistical γ rays and E2 rotational γ rays (whose properties were taken from measured data or from standard estimates [15]). Values for Γ_{rot} and Γ_μ had the form: $0.0033I(E^*)^{1/4}$ and $0.029(E^*)^{3/2}$, respectively. These values are reasonably close to standard estimates [7,15]. We used P_{nar} from Eq. 1 and in order to fit all the gates with a single simulation we took $(v/d)^2$ proportional to E^{*3} (the dependence expected in leading order, *i.e.* in mixing two-particle-two-hole states) and adjusted the coefficient to fit the intensities of the narrow components. When E^* is less than 0.2 MeV we make the γ rays discrete, for which we randomly select a band from among the lowest 2 or 3 bands that are known to very high spins in each of the three Yb nuclei.

The data (black) and simulations (red) from this work

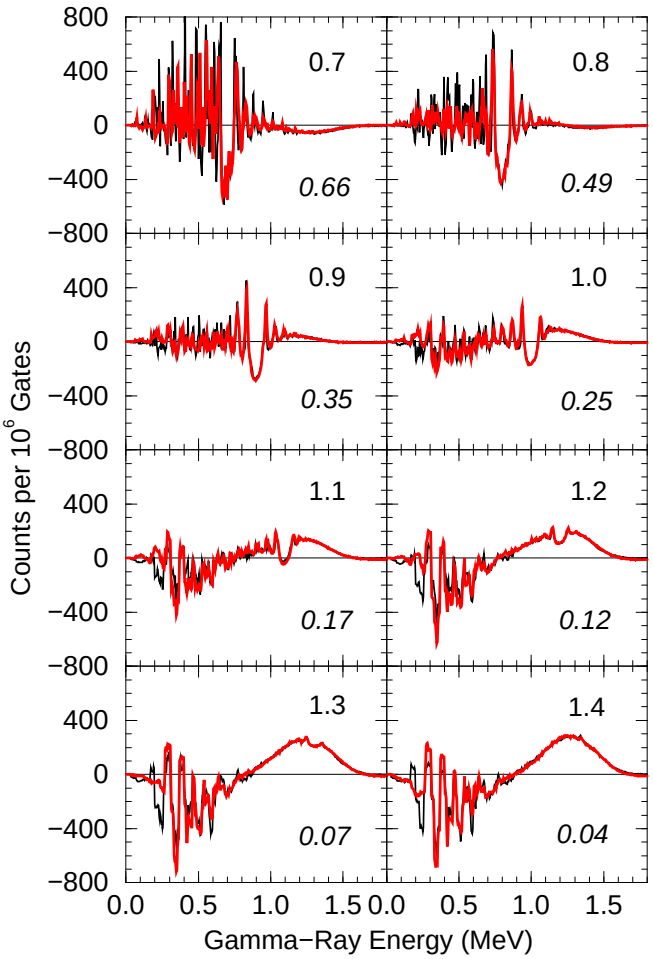

FIG. 3. The data (black) and simulation (red) spectra (see text) are treated identically. The gate energy in MeV is at upper right in each plot and the P_{nar} value is at lower right.

are shown in Fig. 3 for eight gate energies. These spectra are all CORs and are what we call "shift-and-add" spectra: the gates cover a 60-keV range consisting of 15 4-keV wide channels. As each gate channel moves up or down, we move the coincident spectrum up or down by exactly the same amount. Thus the gate always occurs at the same channel in the coincident spectra and we have 4-keV resolution for gate-related effects, whereas other effects tend to be smeared out. This is what we want.

For the higher-energy gates in Fig. 3 there is a broad peak that is a combination of the feeding and rotational correlations. This broad peak becomes smaller as the gate gets lower in the feeding region and actually becomes negative in the lowest two gates which are below all the feeding. In our previous work we called this negative correlation the secondary feeding correlation [13] and used it to get information about the feeding.

Superposed on this broad feature is a narrow valley and ridge structure which gets progressively larger as the gate energy decreases. In detail this structure arises because a de-exciting rotational band emits a very regular set of γ rays (like a picket fence) and gating on one of these results in a spectrum missing this energy - *i.e.* with a valley. The transitions adjacent to the gate are seen as ridges which continue away from the gate energy as long as the population stays in the band and the γ rays are not smeared out in energy. This is what we have called the narrow structure whose intensity indicates how much of the population enters and decays via the same component of the wave function. (Note that these structures can be easily resolved although, due to the high level density, individual γ rays above $\sim$1 MeV are largely unresolvable using present detectors.) Early studies of this narrow component showed it was a separate structure superposed on the rotational-damped spectrum and rough measurements of its the intensity were made, in general agreement with the present values [16].

Measurements of the intensity of this narrow structure are simple and reliable. They do not require identifying separately the compound-damped and discrete γ rays. Both of these γ-ray types arise from events that enter and decay via the same component of the wave function and they produce similar structures in the spectrum. Thus, measuring this intensity is much easier and more reliable than measuring Γ_μ, for example, which requires not only identification of the above γ-ray types but also a knowledge of the E^* distribution from which the γ rays are emitted. In fact, measuring the intensity of this narrow structure does not require use of a simulation code provided: Γ_μ is less than about 100 keV (usually the case), the statistical γ rays are subtracted, and the spectrum is unfolded to remove Compton-scattered γ rays. Our simulation code takes account of all these things.

To measure v/d we ensure that the simulation fits the data (*e.g* Fig. 3) and then record for each gate the fraction of the rotational γ rays that make up the narrow component (*i.e.* the compound-damped and discrete γ rays). This is the average P_{nar}, and we then solve Eq. 1 for the average v/d. This can be done for any gate energy and width and there is very little change with gate width up to the 60 keV width we use. Eight values of P_{nar} are given on Fig. 3 and a ninth value of 0.82 was measured for a 0.6 MeV gate. The uncertainties on these values are estimated to vary from $\sim$10% for the lowest gate (0.6 MeV) to $\sim$30% for the highest. All nine v/d values are given on Fig. 4 and the uncertainties corresponding to those on P_{nar} are all $\sim$20%. At the low gate energies the resolved discrete lines become strong and we do not always reproduce these well because we include only 2 or 3 bands per nucleus. This should have little effect on our P_{nar} values. Another problem is that our simulation indicates there should be extensive motional narrowing [7], especially at the highest γ-ray energies. This would affect Γ_{rot} but should not affect P_{nar} and we have not included motional narrowing in this simulation.

The random matrix described can be diagonalized for any v/d. The NND and Δ_3 statistics of the resulting

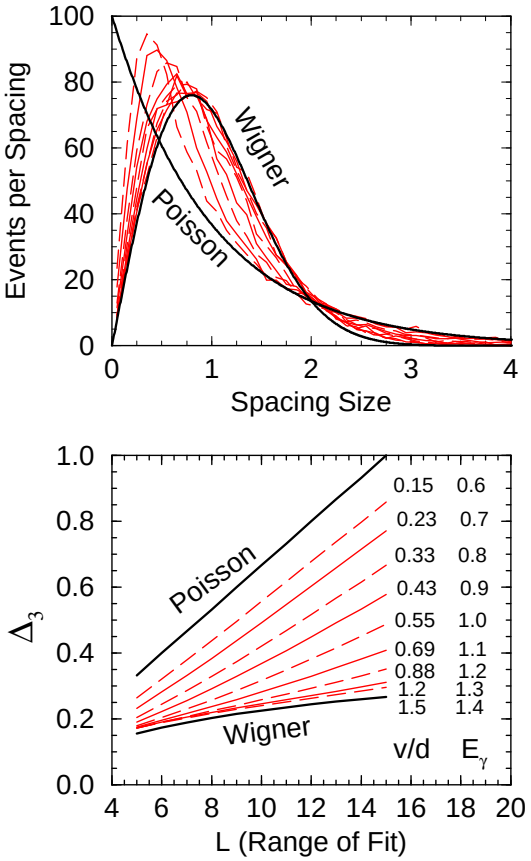

FIG. 4. The distributions, NND (upper) and Δ_3 (lower), for the measured v/d values (indicated) together with the Poisson and Wigner limits (heavy lines). Starting with the first gate alternate gates are dashed to help distinguish them.

levels can then be evaluated. The NNDs are shown in the top part of Fig. 4 for the v/d values we have measured and the Δ_3 statistics curves are shown in the lower part of the figure. Our measured points span the onset of chaotic behavior in these nuclei as indicated by these measures. The behavior becomes chaotic as v/d becomes $\sim$1 as has been pointed out [17]. Of course, a single average v/d value cannot give a complete description of the nuclear behavior: we cannot tell, for example, whether the spread in v/d values is small or large. Nor can we get details about the energy region over which the levels are mixed - we see only the behavior given by the average v/d value. However, our procedure gives a simple and direct measure of the chaos-to-order transition along the average de-excitation pathways in these nuclei.

The simulation can provide much more information. The average P_{nar} values have been discussed until now because they do not really depend on the simulation. Results from the simulation indicate that there is a large spread in E^* for the γ rays in each gate and since v/d depends on E^*, there is also a large spread in v/d values. It would be more meaningful to relate v/d to E^* and this can be done through the simulation. Since the simulation takes P_{nar} from Eq. 1 and v/d depends only on E^*, we can derive an analytic formula for E^*:

$$E^* = 0.91[(1 - P_{nar})/P_{nar}]^{1/3}. \quad (2)$$

The values for E^* vary from 0.5 to 2.6 MeV for our gates; however, they depend on details of the simulation (*e.g.* the E1 and/or E2 transition probabilities), resulting in uncertainties that are difficult to evaluate at present.

This is a new way to explore the order-to-chaos transition in nuclei. It looks directly at a property of the wave function rather than at level spacings and can often be used where measuring the energy-level spacings is not possible. There are two obvious ways to extend these measurements. The first is to use experimental tags (some kind of channel selection) to define more specific decay pathways and thus provide better information on variables like E^*. The second is to make the simulations better and more reliable so we can extract and use more information from them. It would also be interesting to look for other correlated quantities (like our γ-ray emissions) that could be exploited in this way to provide information on chaotic behavior or other properties.

This work has been supported in part by the U.S. DOE under Contract No. DE–AC03–76SF00098. We thank Sven Åberg for helpful discussions on this subject.

[1] O. Bohigas, et al., Phys. Rev. Lett. **52**, 1 (1984).
[2] F.J. Dyson and M. Mehta, J. Math. Phys. **4**, 701 (1963).
[3] O. Bohigas et al., Nucl. Data for Sci. and Technology, K.H. Böchhoff (ed.), Reidel, Dordrecht, p. 809 (1983).
[4] J.D. Garrett et al., Phys. Lett. **B392**, 24 (1997).
[5] S.G. Nilsson, Mat. Fys. Medd. Dan. Vid. Selsk **29**, no. 16 (1955).
[6] S. Åberg, Prog. Nucl. and Part. Phys. **28**, 11 (1992).
[7] B. Lauritzen, T. Døssing, and R.A. Broglia, Nucl. Phys. **A457**, 61 (1986).
[8] M. Matsuo et al. Phys. Lett. **B465**, 1 (1999); Nucl. Phys. **A649**, 379c (1999); Nucl. Phys. **A557**, 211 (1993).
[9] B.R. Mottelson, Nucl. Phys. **A557**, 717c (1993).
[10] V. Zelevinsky, Ann. Rev. Nucl. Part. Sci. **46**, 237 (1996).
[11] A. Bohr and B.R. Mottelson, *NuclearStructure*, vol. 1, p. 304, New York, Benjamin, (1969).
[12] P. Persson and S. Åberg, Phys. Rev. **E52**, 148 (1995).
[13] F.S. Stephens et al., Phys. Rev. Lett. **88**, 142501, (2002); AIP Conf. Proc. **656**, 40 (2002).
[14] O. Andersen et al., Phys. Rev. Lett. **43**, 687 (1979).
[15] T. Døssing and E. Vigezzi, Nucl. Phys. **A587**, 13 (1995).
[16] F.S. Stephens et al., Phys. Rev. Lett. **58**, 2186 (1987); Phys. Rev. Lett. **57**, 2912 (1986).
[17] S. Åberg, Phys. Rev. Lett. **64**, 3119 (1990); P. Jacquod and D. Shepelyansky, Phys. Rev. Lett. **79**, 1837 (1997).